CARBONIC ANHYDRASE 6 AS A MARKER FOR FLAGELLAR ASYMMETRY IN *Chlamydomonas reinhardtii*

by

DIPNA VENKATACHALAM

(Under the Direction of Karl F. Lechtreck)

ABSTRACT

Cilia are cylindrical appendages that protrude out of the cell. *Chlamydomonas reinhardtii* has 2 cilia which are named as *trans* and *cis* with respect to their location from eyespot. The trans cilium extends from the older, mature basal body while the cis cilium extends from the daughter basal body. The axonemes of the two flagella have known to demonstrate opposite beating pattern in response to free Ca^{2+}. We report here for the first time a biochemical marker – Carbonic anhydrase 6, that preferentially localizes in the *trans* flagellum, a asymmetry established during ciliogenesis. We show that both IFT and BBSomes are required for the protein to maintain its asymmetric distribution. We propose that CAH6, a biochemical marker for cilia asymmetry contributes towards the functional difference between the *cis* and *trans* and explore the mechanisms utilized by the cell to establish this asymmetry.

INDEX WORDS: Cilia, asymmetry, carbonic anhydrase, IFT, BBSome

CARBONIC ANHYDRASE 6 AS A MARKER FOR FLAGELLAR ASYMMETRY IN *Chlamydomonas reinhardtii*

by

DIPNA VENKATACHALAM

B.Tech, SRM University, 2015

A Thesis Submitted to the Graduate Faculty of The University of Georgia in Partial Fulfillment of the Requirements for the Degree

MASTER OF SCIENCE

ATHENS, GEORGIA

2019

CARBONIC ANHYDRASE 6 AS A MARKER FOR FLAGELLAR ASYMMETRY IN

Chlamydomonas reinhardtii

by

DIPNA VENKATACHALAM

Major Professor:	Karl F Lechtreck
Committee:	Jacek Gaertig
	Daichi Kamiyama
	Vasant Muralidharan

Electronic Version Approved:

Suzanne Barbour
Dean of the Graduate School
The University of Georgia
May 2019

DEDICATION

Dedicated to Amma, Appa and Neo, whose unconditional love and support inspires me to be the best version of myself.

ACKNOWLEDGEMENTS

First and foremost, I would like to thank my mentor and guide Karl Lechtreck. His incredible work ethic, passion for biology and research is something I hope to achieve during my career. He has been extraordinarily supportive during this journey of mine and I am extremely grateful for it. Next, I would like to thank the members of my committee, Jacek, Daichi and Vasant. Even though we didn't meet often, their insights have been extremely valuable. I would also like to thank my professor back in India, S.Thyagarajan who helped me nurture this passion for cell biology.

I would like to thank all the members of my lab, Ilaria, Peiwei, Aaron, Jenna and Jin. You guys made the lab a warm and welcoming space and I never felt out of place with you all. I would especially like to mention my sounding board Ilaria and my screaming partner Jenna, our time during workout and conversations in lab is something I will thoroughly miss. To our newest lab member Kewei, I have thoroughly enjoyed being your co-TA and a fellow classmate. We have had some interesting discussions together. I truly appreciate how close-knit of a group we all are.

To my friends in Athens, Riju, and Penny – you both have been the perfect combination of a senior graduate student, someone I could confide in with or just unwind. Your guidance and motivation were always there whenever I needed it. To Mayukh and Bratati, I thoroughly enjoyed spending time with the two of you. Thank you for making Athens feel like home.

I would also like to thank my family here in the United States of America. Travelling to a foreign country seemed a bit daunting at first, but with their love, support and confidence the transition was seamless. To my best friend and the rock in my life, Swetha Anandhan, who moved

to the US the same time as me, having you here in this country to have my back has been reassuring. Thank you for your guidance and early morning pep talks.

Finally, I would like to thank my parents. Their boundless love and support have made this dream of mine come true. My mother has always been my rock and my shoulder to cry on and honestly, I don't think I would have the courage and confidence to move to another country if not for her. To my father, my pillar of support, I wish you were here to witness this dream of ours. I have made it this far in life with your love and blessings and I miss you every single day.

I would sincerely like to thank each and every one of you for being a part of this incredible journey of mine.

Thank you.

TABLE OF CONTENTS

Page

ACKNOWLEDGEMENTS v

LIST OF FIGURES viii

CHAPTER

1 Introduction and Literature Review 1

1.1 Cilia: Functions and ciliopathies 1

1.2 Cilia: Ultrastructure and protein transport 1

1.3 Cilia: Asymmetry and *Chlamydomonas* as a model organism 3

2 Results 6

2.1 CAH6-mNG has an asymmetric distribution in *Chlamydomonas* flagella 6

2.2 Loss of CAH6 does not affect flagella length, swimming speed and phototactic ability of Chlamydomonas 8

2.3 Loss of IFT disturbs the asymmetric distribution of CAH6-mNG Chlamydomonas flagella 9

2.4 CAH6-mNG distribution in *uni-1* and *vfl-2* 11

3 Discussion 12

4 Materials and Methods 18

REFERENCES 23

LIST OF FIGURES

Page

Figure 1: The Asymmetric Distribution of CAH6 in *Chlamydomonas* flagella.....7

Figure 2: Loss of CAH6 does not have a severe phenotype in Chlamydomonas 8

Figure 3: IFT is required by CAH6 to maintain its asymmetric flagella distribution 10

Figure 4: CAH6 is present in *uni-1* flagella and has no discernible pattern of localization in *vfl-2* ..…….12

1.Introduction and Literature Review:

1.1 Cilia: Functions and ciliopathies

The eukaryotic cilium is a highly conserved organelle that is characterized by its microtubule-based axoneme originating from the basal body and is enclosed by a ciliary membrane [1]. Cilia participate in a range of functions which can be broadly classified into either functioning for motility or sensing. Motile cilia help cells navigate towards more favorable photosynthetic conditions (light, chemicals) as in Chlamydomonas or to find prey, like in Stentor. Cilia in multiciliated cells beat in a coordinated fashion to clear the pathways from debris and mucus (human trachea, human fallopian tube), to create physiological fluid movements (cerebrospinal fluid in mouse brain ventricles) [2] and to establish left-right symmetry. Immotile primary cilia enable cells to respond to a variety of extracellular stimuli by functioning as a center for a number of signaling pathways. Signaling cascades including Hedgehog and GPCRs have been known to originate in the primary cilia [3]. Cilia gained popularity and emerged as an essential organelle in the past decades when its dysfunction was implicated in a myriad of diseases collectively referred to as ciliopathies. Due to its ubiquitous nature, dysfunction of cilia manifests as a spectrum of characteristics namely retinal degeneration, renal disease, cerebral anomalies, obesity, and skeletal dysplasia. These features are common among ciliopathies as the predominant organs affected by cilia dysfunction are the kidney, liver, eye, and brain [4].

1.2 Cilia: Ultrastructure and protein transport

The cilium lacks ribosomes yet requires proteins for its assembly and maintenance. This obstacle is overcome by a bidirectional protein transport system known as intraflagellar transport (IFT)

carried out by protein complexes termed IFT trains [5]. IFT trains are comprised of repeating large multi-protein subcomplexes (IFT-A and IFT-B) that function as cargo carriers. These IFT subcomplexes move along the microtubule with the aid of motors kinesin-2 and dynein 1b for anterograde (base to tip) and retrograde (tip to base) transport respectively. The anterograde trains and their cargo are assembled at the IFT pool present at each basal body and then enter the cilium. At the tip, the cargoes dissociate while the IFT subcomplexes and the motors undergo a rearrangement that enables their movement back to the base for recycling or degradation. Proteins that are to be exported from the cilium associate with the retrograde trains [6-9].

IFT trains carry a wide variety of proteins, yet are composed of just 22 different protein. Occasionally cargo adaptors, associate with IFT trains to enable them to carry specific cargoes to carry out its full transport function. One such adaptor is an eight-subunit complex referred to as the BBSome. Mutations in the genes encoding these proteins leads to a rare ciliopathy in humans – Bardet-Biedl Syndrome, hence the name of the complex. The BBSome acts as an adaptor primarily for the export of membrane and membrane associated proteins from the cilium [10, 11].

Present at the interface of cytoplasm and cilium is the transition zone (TZ) which behaves as a size-dependent selective barrier, analogous to the nuclear pore complex. The transition fibers and regulatory proteins that constitute the transition zone, control the movement of soluble proteins between the cytoplasm and cilium, allowing small (40-70 kDa) protein complexes to diffuse in and out of the cilium, making diffusion another method of transport of small protein complexes in cilium [12, 13].

On the proximal end of TZ, the basal body is located which is composed of the triplet microtubules, acting as a scaffold for the nine-fold symmetry maintained by the axoneme. *Chlamydomonas* contains three generations of basal bodies, a pair of non-flagellated

granddaughter, which during mitosis transform into daughter basal body. The daughter basal body, which during the next round of cell division is upgraded to the mother basal body. The younger basal body nucleates the *cis* cilium while the parental one nucleates the *trans* cilium [14, 15]. The daughter basal body is connected to the eyespot by the same bundle of microtubules thus placing the eyespot closer to the *cis* cilium as compared to the *trans* cilium.

Enclosing the cilia is the ciliary membrane that is contiguous with the plasma membrane but has a distinct protein and lipid composition that is affluent with sterols, glycolipids, and sphingolipids. This highly enriched lipid composition suggests the possibility of an abundance of lipid rafts in the cilium, for recruiting and retaining ciliary membrane proteins [16, 17]. Thus, there exists a mechanism by which the proteins and lipids are targeted,recognized, and sorted to the cilia.

1.3 Cilia: Asymmetry and *Chlamydomonas* as a model organism.

For protists, having asymmetrical flagella in terms of ultrastructure and function is not unconventional. The key feature of heterokonts (e.g. *Ochromonas*) flagella is the presence of two structurally and functionally distinct flagella on each cell: a short and smooth flagellum and a longer flagellum with mastigonemes. [18]. In multicellular animals, depending on the mélange of factors expressed, the type of cilia varies between cells [19-21]. On the contrary, isokonts (*Chlamydomonas, Anaeramoeba*) have flagella of equal length and morphology [22, 23]. In mammalian cells, when more than one cilium is present, the cell first establishes the immotile cilia hence referred to as primary cilium, followed by the development of numerous motile cilia [24, 25].

Our model organism, *Chlamydomonas reinhardtii* is a unicellular biflagellate that has been used extensively to study eukaryotic flagella. The wide range of biochemical and imaging tools present allows for studying the unanswered aspects of flagellar assembly in *C. reinhardtii*. The

haploid genome and a wide array of mutants present in the large open source Chlamydomonas mutant library generated by the Chlamydomonas Library Project (CLiP) makes it an organism of choice in the ciliary biology community [26, 27].

C. reinhardtii is bilaterally symmetrical except for the presence of a singular eyespot. The eyespot, a photosensory organelle that is responsible for the directional light perception, is located asymmetrically at the periphery of the cell via a bundle of four microtubule roots to the daughter basal body (D4). A 300,000 Da protein, Mlt1 was found to localize exclusively in these D4 microtubules putatively helping in the positioning of the eyespot onto these tubules [28]. This gives rise to a rotational asymmetry wherein the flagellum closer to the eyespot is known as *cis* while the one farther away is *trans* [29].

Furthermore, in reactivated cell models (cells that are stripped of their membrane and treated with ATP) when flagella is exposed to low amount of free Ca^{2+}, the axonemes beat highly asymmetrical to each other [30]. Additionally, there exists the Chlamydomonas mutant *uni-1*, which is uniflagellate with most (>95%) cells possessing only the *trans* flagellum. This demonstrates the ability of the cell to coordinate flagella development with the position of eyespot or the age of the basal body[31].

These studies together lend support to the hypothesis that the two flagella may be compositionally different and points towards a mechanism utilized by the cell to differentiate between them. However, biochemical markers to demonstrate this compositional difference have yet to be identified. Here, we show that CAH6 (Carbonic anhydrase 6) prefers to localize in the *trans* cilium, the first biochemical evidence for flagella asymmetry in *Chlamydomonas*. CAH6, akin to other carbonic anhydrases, participates in the carbon concentrating mechanism in photoautotrophs by reversibly catalyzing the conversion of CO_2 to bicarbonate and its subsequent

conversion to CO_2 when in the proximity of Rubisco [32]. The carbon concentrating mechanism kicks in as the survival mechanism enabling carbon fixation by the cells at low CO_2 conditions, in order to survive and proliferate [33]. We now try to understand the functional significance of the asymmetric distribution of this protein and the molecular basis of its establishment.

2. Results

2.1 CAH6-mNG shows an asymmetric distribution in the *Chlamydomonas* flagella

Previously, we had shown that Phospholipase-D (PLD) and adenosine 5'-monophosphate activated protein kinase (AMPK) – two membrane-associated proteins, accumulate in the flagella while CAH6- another membrane associated protein gradually depletes from the flagella in *bbs* [11]. To understand the role played by BBSome in the transport of these proteins, we tagged both PLD and CAH6 with mNeonGreen (mNG) on the C-terminal end. The N-terminal of these proteins is dual lipidated with a myristoyl and palmitoyl group attached to the second amino acid - glutamine at and the third amino acid - cysteine respectively. These lipid moieties are implicated in the targeting and entry of these proteins in the cilium [34-36]. Using Total Internal Reflection Fluorescence Microscopy (TIRFM) we observed that CAH6-mNG asymmetrically distributes between the two flagella (Fig. 1A). We noted that CAH6 always preferentially localizes to the *trans* flagellum (the flagellum further away from eyespot) in 97.4 % of wild type cells analyzed (n=39). Interestingly, the asymmetry of CAH6-mNG is disturbed in the *bbs4* mutant (Fig1B). A preference for *trans* flagellum was observed in 43% of the *bbs4* cells of the 62 cells analysed. In about 37% cells we observed the opposite pattern of distribution was observed i.e. the amount of CAH6-mNG in cis was greater than that is *trans*. This is unsurprising as the axonemes of the *bbs* mutants lose their asymmetric response when exposed to free calcium ions as compared to wild type. To further understand the kinetics of CAH6-mNG transport, we performed Fluorescence Recovery after Photobleaching (FRAP). CAH6-mNG reestablished its asymmetric distribution in

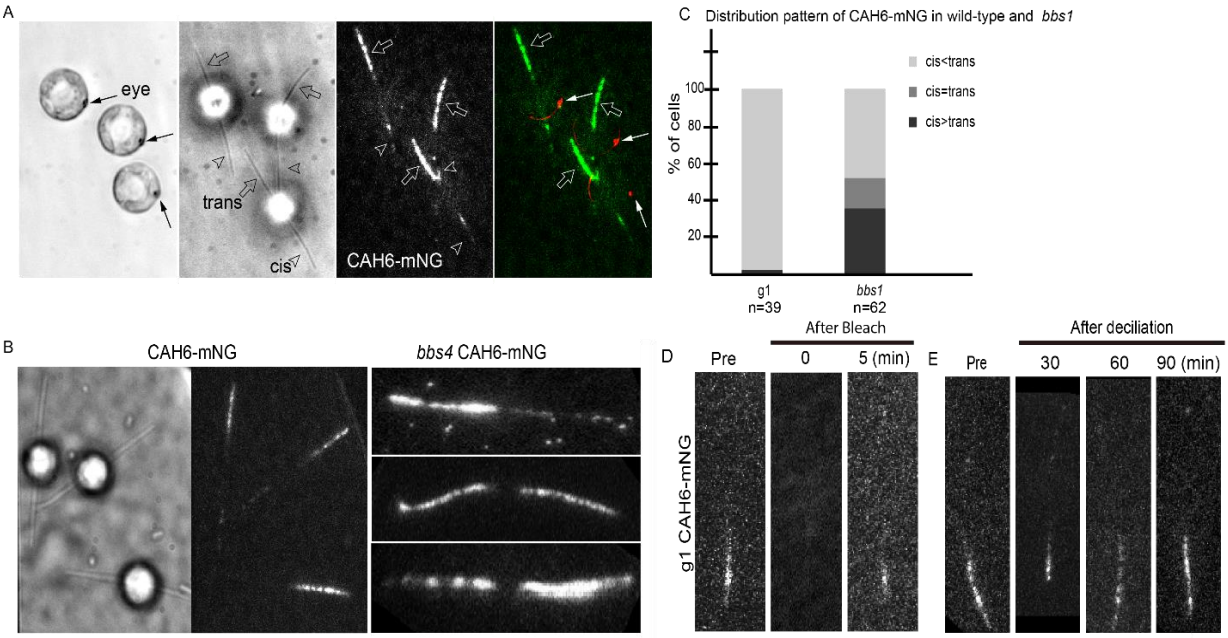

Figure 1: CAH6-mNG localizes preferentially in the *trans* cilium which is disturbed in the absence of BBSomes (A) DIC and TIRFM images showing the location of the eyespot(red) and the localization of CAH6-mNG (green) with respect to it in wild-type cells. The filled arrow points to the eyespot, the empty arrow points to the *trans* cilium and the empty arrowhead points to the *cis* cilium (B) DIC and TIRFM images showing the location of the eyespot(red) and the absence of asymmetry of CAH6-mNG (green) in *bbs4*. The second panel demonstrates the three distribution patterns observed. (C) Quantitative representation of the asymmetry observed in wild-type (n=39) and *bbs4* (n=62). (D) FRAP analysis on wild type cells showing recovery of signal at 5 mins after photobleaching. (E) TIRFM images of wild type cells showing the localization of cah6-mng at various time points after deciliation. We see the asymmetry is established as the cilia regenerates. n= number of cells analyzed.

five minutes in wild-type cells showing a continuous exchange of CAH6-mNG between the cilium and cell body (Fig 1D). Next, to investigate if this asymmetry is established during the initial assembly of cilia

or occurs as the cilia ages, we utilized the ability of Chlamydomonas to regenerate a full-length cilium in ~60 minutes. After deciliation, we observe that in a regenerating cilium (30 minutes) the asymmetry is already established. We next used immunofluorescence to observe the localization of endogenous CAH6 (data not shown) and observed background signal in our mutant. We used the same antibody used to identify the localization of CAH6 in chloroplast by immunogold electron microscopy [37]. This antibody while able to work in western blot to detect endogenous CAH6 (Fig 2C) in isolated cilia was not robust enough to detect the Neon-Green tagged version

(not shown) or for immunofluorescence experiments. We suspect that the antibody was raised against the C-terminal hence could not detect the tagged version due to the presence of the NG tag on the C-terminal. We now are in the process of generating a new antibody for CAH6. Thus, the asymmetric distribution is seen only for the –NG tagged version of CAH6 expressed in both wild type (with endogenous CAH6) and in the cah6 mutant (only CAH6-mNG present).

2.2 Loss of CAH6 does not affect flagella length, swimming speed and phototactic ability of *Chlamydomonas*

To identify the role of the CAH6 and better understand its unique distribution we obtained a

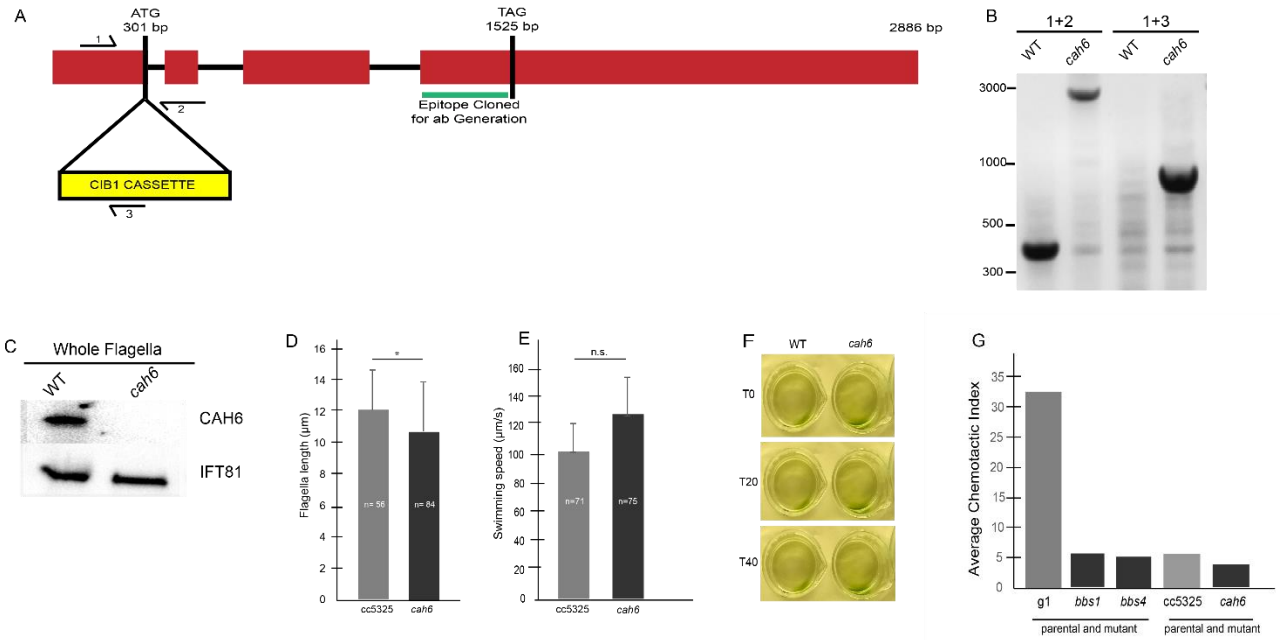

Figure 2: Loss of CAH6 does not have a severe phenotype in *Chlamydomonas*. (A) A schematic representation of CAH6.The primers used to identify the mutant are shown. The site of insertion for the mutation has been identified at the end of exon 1. (B) Identification of the *cah6* with PCR using the primer pairs (top). (C)Western blot analysis of the isolated flagella from wild-type and *cah6* cilia. The antibodies used to probe were anti-CAH6 and anti-IFT81 as a loading control. (D-G) Phenotypic analysis of the mutant by assaying the flagella length, swimming speed, phototaxis and chemotaxis between the parental (cc5325) and *cah6*.

putative insertional mutant in CAH6 gene from the CLiP mutant library[27]. We confirmed the insertion site of the CIB1 cassette (confers paromomycin resistance) to be directly after the start

codon of CAH6 (Fig 2A and B). Using western blotting, we also confirmed that *cah6* is a null mutant (Fig. 2C). We compared several *Chlamydomonas* flagella characteristics such as flagella length and swimming velocity between the mutant and its parental strain (cc-5325) (Fig 2D and E) but failed to observe a discernible phenotype. We also looked at the phototactic (Fig 2F) and chemotactic ability (Fig 2G) of the strains, the latter was carried out in collaboration with Dr.S.J Sim (Korea University) using an agarose gel based microfluidic device. The chemotactic index was calculated by calculating the ratio of number of cells present in the observation region in response to 30mM sodium bicarbonate to that observed in response to the negative control. We discovered that the parental strain in itself is defective in chemotaxis. Thus, to determine the true phenotype of *cah6* we are in the process of repeatedly backcrossing *cah6* with the wild-type strain (g1). This will help us eliminate other possible mutations and place CAH6 into a typical control background rather than the parental strain.

2.3 Loss of IFT disturbs the asymmetric distribution of CAH6-mNG in *Chlamydomonas* flagella

In-vivo imaging of CAH6-mNG in flagella revealed that the majority of its movement inside the cilia is by diffusion, with occasional events of IFT. However, since CAH6- is comparatively a protein of low abundance, this does not exclude that possibility that IFT establishes or maintains the flagellar asymmetry of CAH6. To determine if IFT contributes to this asymmetry, for example by depleting the *cis* cilium of CAH6, we expressed CAH6-mNG in *fla10*-1. *fla10*-1 are temperature sensitive mutants of kinesin II which, at their restrictive temperature (32°C) stops IFT. Using TIRFM we observed that on incubation of fla10-1 CAH6-mNG cells at 32°C for 3 hours, t CAH6-mNG requires IFT to maintain its asymmetry. We next determined the levels of the endogenous CAH6lost (n=16) while the wild-type cells retained the asymmetry (Fig 3A). This

suggests that CAH6 requires IFT to maintain its asymmetry (n=16). We next determined the levels of endogenous CAH6 in the wild-type and *fla10-1* to understand how the loss of IFT affects the

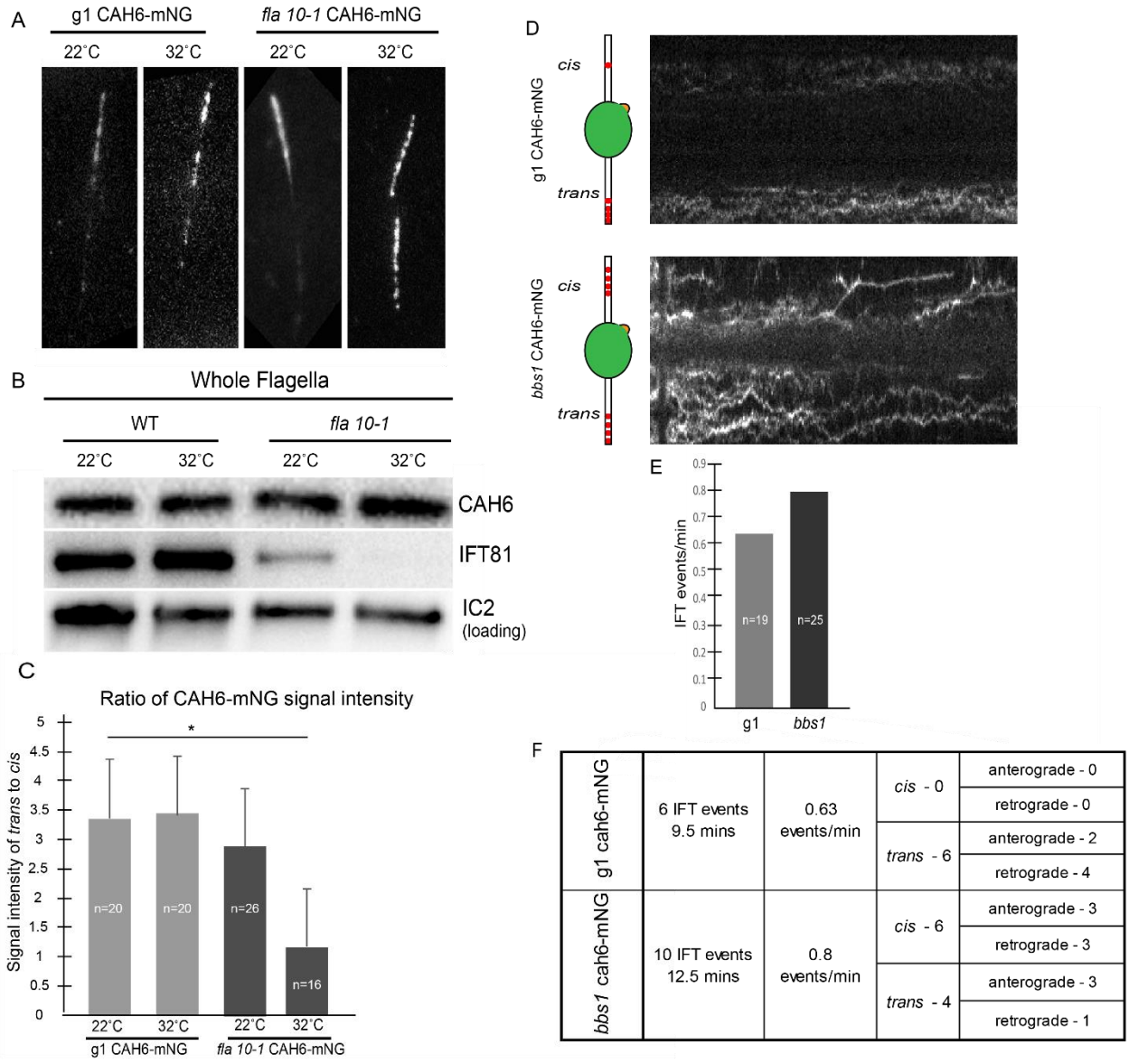

Figure 3: IFT is required for CAH6 to maintain its asymmetric flagella distribution. (A) TIRFM images showing the distribution of CAH6-mNG in g1 and *fla10-1* at the permissive (22°C) and restrictive temperature (32°C). (B) Western blot of the isolated flagella of wild-type and *fla10-1* cells incubated and the temperature (top) for 3 hours and probed with anti-CAH6. Anti-IFT81 was used as the *fla10-1* control and its absence at the restrictive temperature confirms shut down of IFT. Anti-IC2 was used as the loading control. (C) Quantitative representation of the ratio of signal intensity of CAH6-mNG in *trans* cilium to the *cis* cilium for wild type and fla10-1 mutants at the two temperatures. (D) Kymograms showing the rare IFT transport of CAH6-mNG in g1 and *bbs1* cells. (E) IFT events observed in g1 and *bbs1*flagella were quantified as events per minute.(F) Table depicting the breakdown of anterograde and retrograde events of CAH6-mNG in g1 and *bbs1* for *cis* and *trans* flagellum individually. n= number of cells analyzed.

presence of CAH6 in the flagella (Fig. 3B). The cells were incubated at 32°C for 2.5 hours and then cilia were isolated. Loss of IFT81 at the restrictive temperature confirms the shut-down of

IFT, and we observe an accumulation of CAH6. The increase of CAH6 at the restrictive temperature suggests that CAH6 export from the cilia by IFT contributes to its asymmetric distribution observed by TIRFM.. We further quantified the ratio of the signal intensities of CAH6-mNG in *trans* to *cis* (Fig. 3C). We observe a 3-fold decrease in the ratio for the *fla10-1* at the restrictive temperature in comparison to the wild-type. The data indicated that IFT is involved in establishing the distribution of CAH6. Next, we quantified the IFT events/min for the wild type and *bbs1* cells (Fig. 3D-E). We observed a slightly higher number of IFT events in *bbs* that were predominantly observed in the *cis* flagellum and in the *trans* flagellum the anterograde events were higher. The near absence of IFT transport events in the *cis* flagellum of g1 is because these cilia are devoid of CAH6. One possible explanation is that CAH6 is exported out by IFT from the *cis* flagella in a BBSome dependent manner.

2.4 CAH6-mNG distribution in *uni-1* and *vfl-2*

There are a number of physical characteristic that can be utilized by the cell to divert CAH6 toward the *trans* flagellum for e.g., age of the cilium, age of the basal body, position or number of the eyespot. To identify this we took advantage of the availability of various basal body mutants. CAH6-mNG was expressed in a uniflagellate mutant (*uni-1*) and in a variable flagella mutant(*vfl-2*) (Fig.4A and 4B). We observed that when only the *trans* flagellum is present as in the case of *uni-1*, CAH6-mNG is present in the flagellum. In the case of *vfl-2* due to segregation defects, the cells have any number of flagella ranging from zero to four and can have one or more eyespots. A consistent pattern of localization of CAH6 with respect to the eyespots position and flagella number was not observed.

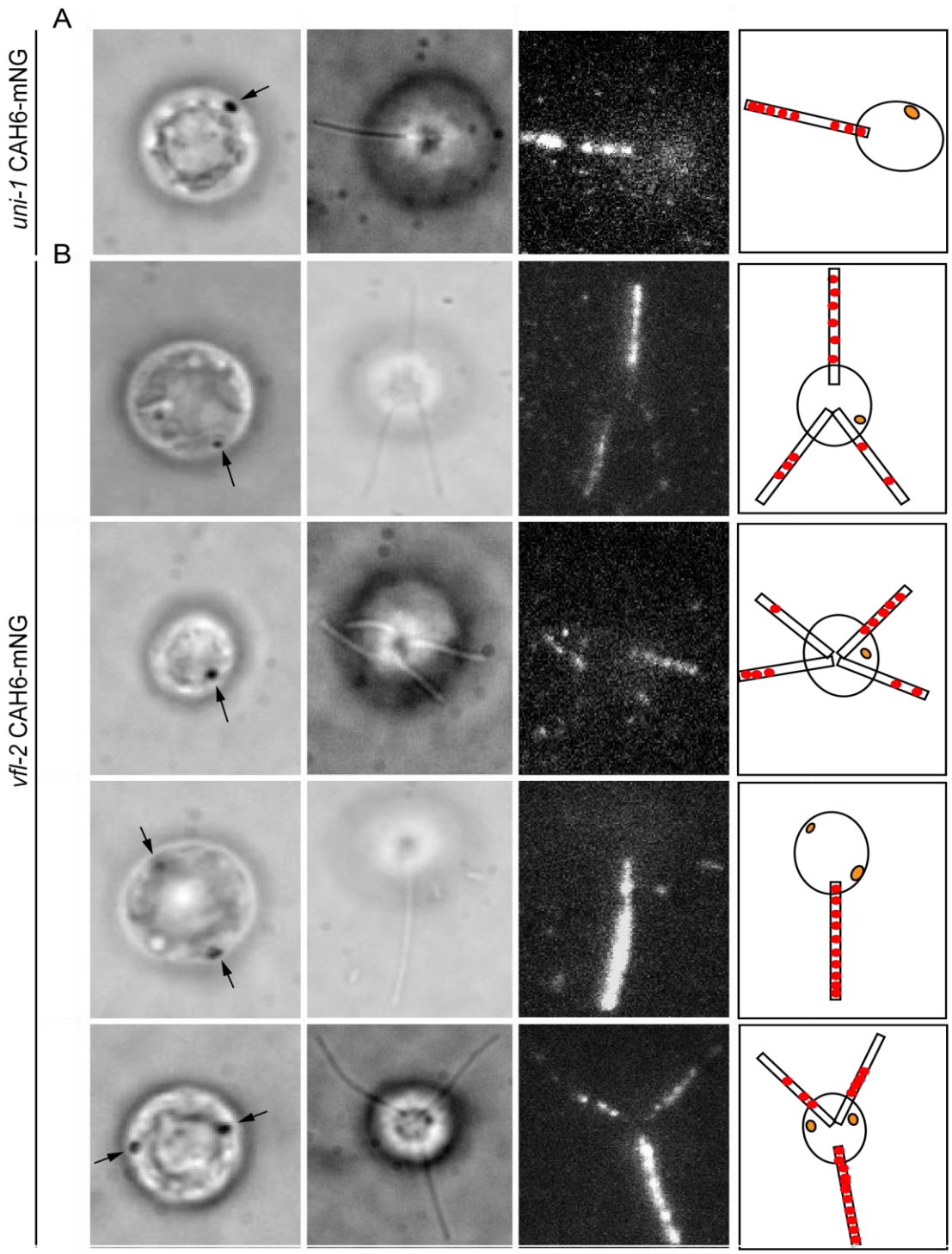

Figure 4: CAH6 is always present in *uni-1* flagella and has no discernible pattern of localization in *vfl-2*. (A) CAH6-mNG always localizes to the *trans* flagella in the uniflagellate mutant, *uni-1* (n=13) (B) Localization pattern of CAH6-mNG in *vfl-2* mutant showing the various combinations of eyespot and flagella number (n=40). The distribution of CAH6-mNG does not seem to follow a clear pattern. Black arrows on the left most panel points to the eyespot

3. Discussion

For long it has been known that heterokont cells establish two distinct cilia, but how the cell achieves this is yet to be understood. Flagella of *Chlamydomonas*, an isokont, are superficially identical but are different in terms of development (age of the basal body they arise from, development of singular flagella in *uni* mutants) and function (axonemal response to $Ca2^{+}$) [29, 30]. Evidence of compositional difference between the two flagella are not yet known and CAH6 is the first biochemical marker identified in *Chlamydomonas* illustrating this difference. With the tools already established in *Chlamydomonas*, genetic and biochemical imaging of CAH6 allows us to utilize it as a tool to understand the means by which a cell proceeds to establish a compositional difference between the two flagella. Studying the transport mechanism of CAH6 will help us elucidate the ciliary targeting of proteins and how the cells control entry of protein in cilia.

Cilia react to multiple environmental signals thus acting as a hub of signaling proteins and their secondary messengers. Defect in the cilia can lead to a group of diseases that falls under the umbrella of ciliopathies such as Bardet-Biedel Syndrome (BBSome). The BBSome helps in the cycling of membrane and membrane associated proteins in the cilia through IFT. In *Chlamydomonas bbs* mutants, the levels of flagellar membrane-associated proteins have shown to be affected. CAH6, a dual lipidated membrane associated protein had been shown to gradually decrease in the flagella of *bbs 4-1* mutants [11]. CAH6 localizes to both the flagella in *bbs* mutants in contrast to its asymmetrical distribution in wild type. This suggests that BBSome plays a role in enabling CAH6 to selectively localize in the trans flagellum. Similarly, when *fla10-1* cells were

incubated at the restrictive temperature to switch off IFT, the asymmetry was lost. Thus, shutting off IFT interfered with the selective localization of CAH6 suggesting its role in maintaining this asymmetry. However, majority of CAH6 diffuses in and out of the cilium yet IFT and BBSome are responsible for its asymmetric localization. One hypothesis could be that CAH6 is specifically depleted from the *cis* cilium by IFT and BBSomes. Analyzing dikaryons of *bbs* CAH6-mNG and g1 CAH6-mNG might help us test this hypothesis. If the re-introduction of BBSomes in the *bbs* deficient cilia helps in restoring the asymmetry originally observed in wild-type our hypothesis might be tested true. Additionally, we know that lack of IFT or BBSome effects the distribution of a large number of proteins. Therefore, the mislocalization of other membrane components could lead to the shift in CAH6 asymmetry. A further study ascertaining interacting partners of CAH6 might help us understand the method of its establishment.

There are a number of characteristics of the transition zone and basal body for example, the age of the basal body, position of the eyespot that could potentially be recognised by IFT to differentiate between the two flagella. These characteristics can be utilized by IFT to preferentially upregulate or downregulate their cargo or the transition zone could have selective permissivity which could be related to the age of the basal body. The two cilia in Chlamydomonas arise from basal bodies of different ages, but the compositional difference between the basal bodies is yet to determined [29, 38] . The eyespot is connected to the daughter basal body by microtubule roots, which could be another element that could help guide IFT away from that particular cilium. Thus, we looked at the localization of CAH6-mNG in two basal body mutants – *vfl-2* and *uni-1*.

vfl-2 lacks centrin and nucleus- basal body connectors thus affecting the centriole duplication and segregation [39]. This leads to cells with flagella number ranging from 0 to 4 with one or more eyespots. The increasing number of variables in *vfl-2* including the presence of

multiple eyespots and their various positions, difference in flagella segregation made it complicated for us to identify a distinct pattern. Thus, we have decided to eliminate as many of these variables using other Chlamydomonas mutants such as the *mlt-1* (multiple eyespots) and *eye-1* (no eyespots). This might help us understand the role the eyespot and/or its location plays in this distribution [40].

uni-1 has a defect in the transition of the triple microtubules to doublet microtubules which has been deemed essential for assembly of flagella. It is likely that this has a severe effect on the younger basal body thus causing a failure of *cis* flagellum assembly while the *trans* cilium is assembled and functional. Thus, seeing if this structural defect in the younger basal body has an effect on CAH6 localization might help us identify or eliminate a factor involved in this selective targeting of CAH6.

Carbonic anhydrases are a family of zinc metalloenzymes that are responsible for the carbon concentrating mechanism (CCM) which helps photoautotrophs to increase the CO_2: O_2 ratio. This enables the cells to acclimatize to environments that have low carbon dioxide concentrations. Carbonic anhydrases have been previously implicated in the regulation of pH, transport of CO_2 and HCO_3^-, ions and maintaining the water-electrolyte balance [41, 42]. In humans, they have been involved directly and indirectly in the metabolic processes such as ureagenesis, lipogenesis, and gluconeogenesis along with production of aqueous humor, cerebrospinal fluid and pancreatic juice [43].

In *Chlamydomonas,* carbonic anhydrases are associated with the pyrenoid tubules in the pyrenoid. The pyrenoid is located in the chloroplast and is brimming with Rubisco, the carbon-fixing enzyme [32]. Out of the twelve carbonic anhydrases present in *Chlamydomonas*, CAH6 is the only one present in the cilia. In response to light, a Ca^{2+} influx is observed in *Chlamydomonas*

[44]. As mentioned before, the two flagella demonstrate opposite response to Ca^{2+} thus helping the cell negatively or positively phototax. *bbs* mutants, lose this asymmetric response to Ca^{2+} hence are unable to phototax. Moreover, the asymmetry of CAH6 distribution is also lost in *bbs* but *cah6* can phototax. This might suggest that CAH6 might contribute to other behaviours in Chlamydomonas. To see if it functions as a carbon sensor, the chemotactic activity of *cah6* expressed in a typical wild-type background needs to be assayed. A lack of severe phenotype can be possibly explained by the redundancy of carbonic anhydrases. This is not unusual as in humans, Carbonic anhydrase 1 is the most abundant non-hemoglobin protein in erythrocytes, yet its absence does not seem to affect the erythrocytes [43]. Determining if CAH6 is functionally active in the cilia and if so its role will help us elucidate the mechanism involved in its selective targeting and confirming that CAH6 is a biochemical marker for the *trans* cilium.

MATERIALS AND METHODS

Strains and culture conditions

C. reinhardtii was maintained in batch cultures in a modified M (minimal media) at 21°C with a light/dark cycle of 14:10 h; larger cultures were aerated and supplemented with 0.5% CO2. The strains used in this study are listed in Table 1

The following strains were used in this study: wild-type (cc-620 and cc-621), cah6 (LMJ.RY0402.174362), bbs4-1(Lechtreck et al.2009), cah6(CAH6FLNG), fla10-1 (cc-1919), vfl-2(cc-1388), uni1(cc-1926),

Identification and characterizarion of C. *reinhardtii cah6* mutant

Primer pairs 1-2,1-3 and 4-5,4-6 were used to map the insertion in the *cah6* mutant. PCR was performed using the BioRad thermocycler using the following cycle conditions: Primer pair 1-3 was used to confirm the location of insertion by sequencing (Genewiz).

Transgenetic strain generation

Primers pair 7 and 8 were used to PCR amplify the coding portions of the CAH6 using CC-620 genomic DNA as a template and the PCR fragment was cloned into the HpaI and XhoI sites of the ipBR vector. This placed CAH6 downstream of the HSP70A-rbcS2 fusion promoter and upstream of the mNG gene the 2A sequence, the zeocine resistance selectable marker and the tubulin terminator [45].

Isolation of cilia and sample preparation

To isolate flagella, cells were concentrated and washed with 10 mM Hepes (pH 7.4) and 10 mL of ice-cold HMS (10 mM Hepes, pH 7.4, 5 mM MgSO4, and 4% sucrose wt/vol) was added gentlyand care was taken that the cells weren't mixed with HMS. Then, 2 mL of dibucaine (25 mM in H2O; Sigma) was added, and cells were deciliated by pipetting on ice. Next, 20 mL of 0.7 mM EGTA (pH 8.0) in HMS were added, and the cell bodies were removed by centrifugation (2,500 rpm, 3 min, 4 °C; Sorvall Legend XTR; Thermo Scientific). The supernatant was underlaid with a sucrose cushion (10 mL of 25% sucrose in HMS) and

centrifuged (2,800 rpm, 4 °C, 10 min) to remove the remaining cell bodies. The flagella were harvested from the supernatant by centrifugation (12,000 rpm, 4°C, 15 min) (Avanti JXN26; Beckman Coulter), resuspended in HMEK+PI (30 mM Hepes, 5 mM MgSO4, 0.5 mM EGTA, 25 mM KCl, 1% protease inhibitor mixture P9599; SigmaAldrich). The isolated flagella were extracted with Nonidet P-40 Alternative (1% final concentration, CAT no. 492016; CalBiochem) for 20 min on ice. The axonemal and membrane+matrix fractions were separated by centrifugation (16,000 rpm, 4 °C, 15 min). Alternatively, flagella were extracted with 1% final concentration Triton X-114 (CAT no. 9036-19-5; Sigma-Aldrich), the axonemes were removed centrifugation (12,000 rpm, 4°C, 10 min), and the supernatant was incubated at 30 °C for 5 min to induce phase separation. The aqueous phase (Matrix)and detergent phase (Membrane) were separated by centrifugation (6,000 rpm, 15 min). The aqueous phase was treated with 1% Triton X-114, the detergent phase was diluted with HMEK+PI, and the phase separation was repeated to yield the final matrix and membrane fractions. The proteins in the membrane fraction were extracted using methanol/chloroform. To the detergent phase, 400uL 100% Methanol was added and vortexed briefly. Next, 100uL of chloroform was added and vortexed again. This was followed by 300uL of water and centrifugation (14,000rpm, 5 min). The top layer was discarded and another 300uL 100% Methanol was added. The sample was centrifuged again and the resultant supernatant was discarded and the pellet was air-dried. All the samples were resuspended in Lamelli's Sample Buffer and incubated at 80°C for 10min.

Antibody purification, production and Western Blotting

Primers 9 and 10 were used to amplify a partial cDNA encoding the first 100 residues of exon 4 of CAH6; after digestion with EcoRI, the fragment was inserted into the EcoRI site of the bacterial expression vector pMAL-cR1(NEB). The vector was then transformed into ElectroTen-Blue Electroporation Competent Cells (Cat # 200159, Agilent Technologies). The cells were grown in 500ml of Rich Medium +glucose and ampicillin (10g tryptone, 5g yeast extract, 5g NaCl, 2g glucose, ampicillin to 100μg/ml per 1L). 0.3mM IPTG was added to the culture when the absorbance at 260nm was around 0.5. The cells were harvested at 5,000 rpm for 20 minutes and resuspended in 20 ml of Column Buffer (20mM Tris-HCl, 200mM NaCl, 1mM EDTA, 1mM DTT). The cells were then lysed using a French press at 20 kPa. The lysed solution was

centrifuged at 15,000 rpm for 20 mins and the supernatant and pellet were separated. The supernatant was run on a PAGE gel, immobilized on nitrocellulose membrane and stained with Ponceau. The strip containing the fusion protein above 50kDa was excised and then blocked with 1%BSA for 1 hour. It was then rotated overnight at 4°C with anti-CAH6 (150ul sera in 350 ul of 1% BSA) antibody provided by J.V. Moroney (Louisiana State University). The strip was washed 4-6 times with 1% BSA. The strip was then incubated in a tube with 100ul of 0.2M Glycine in1mM EDTA at pH 2.16 for 2 mins to release the bound antibody. The extracted antibody was neutralized by adding it to a tube with 100uL of 0.6% BSA, 0.2M Tris in 1X TBST. 0.01% Sodium azide was added to the purified antibody and then used at a dilution of 1:500. The same supernatant was used to purify the fusion protein by affinity purification. 2mL of amylose resin was added to a column and washed with 10mL of column buffer at a flow rate of 1mL/minute. The supernatant was loaded and incubated for 10 minutes and then washed with 15mL of column buffer. The elution buffer (20mM Tris-HCl, 200mM NaCl, 1mM EDTA, 1mM DTT, 10mM Maltose) was then passed through the column and 10 samples of 0.5mL were collected. The purified fusion protein was used for antibody production in rabbits (Pocono Rabbit Farm & Laboratory). Western blots were developed using anti-mouse and anti-rabbit IgG conjugated to horseradish peroxidase (Syngene Femto) and chemiluminescence images were captured and documented using a UVP Autochemi Bioimaging System (Cambridge, UK). Other polyclonal antibodies used were FAP12(1:1000), IC2(1:1000) and IFT-81(1:500)

Mating experiments

To generate gametes, cells were grown for 10 d on Tris-acetate-phosphate medium plates [46] and resuspended in modified M medium without nitrogen (10 ml/plate; M-N), and the suspension was incubated overnight in constant light with gentle agitation. The next morning, cells were incubated in 20% M-N supplemented with 10 mM Hepes. Smaller aliquots of gametes were mixed every 30 minutes and then subsequently checked for their vis-à-vis configuration. When the configurations were attained, larger aliquots of gametes were mixed and left under constant light without shaking for 4 hours. The gametes were plated on phytagel plates () and let dry under light overnight. The following day, the plates were wrapped in aluminum foil and incubated in dark for 4 weeks. After 4 weeks, the plates were placed in -20°C. 2 days

later, the plates were let thaw under, after which they were placed under constant light.

Immunofluorescence microscopy

Fresh grown cells were harvested (3 min at 2,300 rpm, at room temperature) and resuspended in ice-cold HMEK (10 mM Hepes, 5 mM MgSO4, 5 mM EGTA, and 25 mM KCl). One aliquot of cells was mixed with an equal volume of 3% formaldehyde + 0.5% Nonidet P-40 in HMEK while the other aliquot had no fixative. The cells were allowed to settle onto poly-l-lysine–coated multi-well slides for 5 min and then submerged into -20°C methanol for 8 min and air dried. The slides were then blocked in 1% BSA/PBS. Purified anti-CAH6 (see above in antibody purification) was used at a dilution of 1:100, 1:20 and 1:1; and anti–acetylated α-tubulin (1:1000, mouse; Sigma-Aldrich). Specimens were incubated overnight at 4°C with primary antibodies in 1% BSA/PBS. Secondary anti-rabbit linked to Alexa Fluor 488 and anti-rabbit linked to Alexa Fluor 568(1:1,000; Invitrogen) were applied for 90–120 min at room temperature. Specimens were mounted with ProlongGold (Invitrogen). Images were acquired using Axiovision software (Carl Zeiss) and an AxioCam MRm camera (Carl Zeiss) on a microscope (Axioskop 2 plus; Carl Zeiss) equipped with a 100× NA 1.4 oil DIC Plan-Apochromat objective (Carl Zeiss) and epifluorescence. Image brightness and contrast were adjusted using Photoshop (CS5.1; Adobe), and figures were assembled using Illustrator (CS5.1; Adobe). Capture times and adjustments were similar for images mounted together. An Axio Imager.Z1 equipped with a 100× NA 1.3 EC PlanNeofluar objective, an Apotome, an axiocam MRm, and Axiovision software (all from Carl Zeiss) was used to obtain optical sections of the immunostained cell shown in Fig. 1 G. Figures were prepared using Adobe Photoshop and Illustrator.

Observation of IFT

IFT in the flagella was observed using TIRFM at RT. Cells in medium allowed to adhere for ~0.25–1 min and covered with a coverslip to form a chamber enclosed by a Vaseline ring. The fluorescence images were captured using a custom-built TIRF microscope based on an inverted microscope (IX71; Olympus) equipped with a Plan-Apochromat 60× NA 1.4 objective (Olympus). Multiline argon/krypton lasers (CVI Melles Griot) provided excitation light at 488 and 568 nm. Both lasers were cleaned up with appropriate MaxLine Laser-line filters (Semrock Inc.). A 488-nm RazorEdge beam splitter (Semrock, Inc.) was used

for the GFP signal. An FF498/581 beam splitter (Semrock Inc.) was used for the GFP/mCherry signals. The resulting two-color emission signals were separated using a custom-built dual-view system equipped with an FF562-Di01 dichroic mirror (Semrock Inc.) and 525/50-nm and 630/69-nm emission filters (Semrock Inc.). Signals were recorded using a back-illuminated electron-multiplying charge-coupled device camera (iXon DV860; Andor Technology). Data were analyzed using ImageJ (National Institutes of Health) and Photoshop.

Measurement of flagellar length and assessment of swimming velocity

Cells were washed and resuspended in fresh M medium and observed by using an inverted microscope. One flagellum each on cells were measured using ImageJ and the average flagella length was calculated. Swimming velocity was measured by tracking images of moving cells recorded by means of bright-field microscopy using a 40× objective, 5× eyepiece and a digital camera incorporating a charge-coupled device. Recorded movies were processed using ImageJ to obtain average swimming velocities

Sequence of Primers used

1-5’ACACTTATCTTACCACACGCGC-3’

2-5’ ACTCCTCCACCATTCTGAGGC-3’

3- 5’TTGCTCGTCGACTTACCTGGC-3’

4-5’-AATTCCTTTCCGTCGCAGGG – 3’

5-5’- CTTGGTCGAACACAATTTCCGC-3’

6-5’- TTGCTCGTCGACTTACCTGGC–3’

7-5’-CGCCTCGAGCTCGGCGCTGCTGCCGCC-3’

8-5’- CGCGTTAACATGGTGAGCGAAGACCGGCG-3’

9-5’CGCGAATTCAAGGCGTTCCCCGGCTTC–3’

10-5’-CGCGAATTCCTACTCGGCGCTGCTGCCG–3’

References

1. Fisch, C. and P. Dupuis-Williams, *Ultrastructure of cilia and flagella - back to the future!* Biol Cell, 2011. **103**(6): p. 249-70.
2. Wan, K.Y., *Coordination of eukaryotic cilia and flagella.* Essays Biochem, 2018. **62**(6): p. 829-838.
3. Nishimura, Y., et al., *Primary Cilia as Signaling Hubs in Health and Disease.* Adv Sci (Weinh), 2019. **6**(1): p. 1801138.
4. Badano, J.L., et al., *The ciliopathies: an emerging class of human genetic disorders.* Annu Rev Genomics Hum Genet, 2006. **7**: p. 125-48.
5. Rosenbaum, J.L. and G.B. Witman, *Intraflagellar transport.* Nat Rev Mol Cell Biol, 2002. **3**(11): p. 813-25.
6. Signor, D., et al., *Role of a class DHC1b dynein in retrograde transport of IFT motors and IFT raft particles along cilia, but not dendrites, in chemosensory neurons of living Caenorhabditis elegans.* J Cell Biol, 1999. **147**(3): p. 519-30.
7. Porter, M.E., et al., *Cytoplasmic dynein heavy chain 1b is required for flagellar assembly in Chlamydomonas.* Mol Biol Cell, 1999. **10**(3): p. 693-712.
8. Pazour, G.J., B.L. Dickert, and G.B. Witman, *The DHC1b (DHC2) isoform of cytoplasmic dynein is required for flagellar assembly.* J Cell Biol, 1999. **144**(3): p. 473-81.
9. Kozminski, K.G., P.L. Beech, and J.L. Rosenbaum, *The Chlamydomonas kinesin-like protein FLA10 is involved in motility associated with the flagellar membrane.* J Cell Biol, 1995. **131**(6 Pt 1): p. 1517-27.
10. Nachury, M.V., et al., *A core complex of BBS proteins cooperates with the GTPase Rab8 to promote ciliary membrane biogenesis.* Cell, 2007. **129**(6): p. 1201-13.
11. Lechtreck, K.F., et al., *The Chlamydomonas reinhardtii BBSome is an IFT cargo required for export of specific signaling proteins from flagella.* J Cell Biol, 2009. **187**(7): p. 1117-32.
12. Breslow, D.K., et al., *An in vitro assay for entry into cilia reveals unique properties of the soluble diffusion barrier.* J Cell Biol, 2013. **203**(1): p. 129-47.
13. Kee, H.L., et al., *A size-exclusion permeability barrier and nucleoporins characterize a ciliary pore complex that regulates transport into cilia.* Nat Cell Biol, 2012. **14**(4): p. 431-7.
14. Dutcher, S.K. and E.T. O'Toole, *The basal bodies of Chlamydomonas reinhardtii.* Cilia, 2016. **5**: p. 18.
15. Wingfield, J.L. and K.F. Lechtreck, *Chlamydomonas Basal Bodies as Flagella Organizing Centers.* Cells, 2018. **7**(7).
16. Lechtreck, K.F., et al., *Cycling of the signaling protein phospholipase D through cilia requires the BBSome only for the export phase.* J Cell Biol, 2013. **201**(2): p. 249-61.
17. Tyler, K.M., et al., *Flagellar membrane localization via association with lipid rafts.* J Cell Sci, 2009. **122**(Pt 6): p. 859-66.

18. Beech, P.L., K. Heimann, and M. Melkonian, *Development of the flagellar apparatus during the cell cycle in unicellular algae.* Protoplasma, 1991. **164**(1-3): p. 23-37.
19. Mukhopadhyay, S., et al., *Sensory signaling-dependent remodeling of olfactory cilia architecture in C. elegans.* Dev Cell, 2008. **14**(5): p. 762-74.
20. Stubbs, J.L., et al., *The forkhead protein Foxj1 specifies node-like cilia in Xenopus and zebrafish embryos.* Nat Genet, 2008. **40**(12): p. 1454-60.
21. Burghoorn, J., et al., *Dauer pheromone and G-protein signaling modulate the coordination of intraflagellar transport kinesin motor proteins in C. elegans.* J Cell Sci, 2010. **123**(Pt 12): p. 2077-84.
22. Taborsky, P., T. Panek, and I. Cepicka, *Anaeramoebidae fam. nov., a Novel Lineage of Anaerobic Amoebae and Amoeboflagellates of Uncertain Phylogenetic Position.* Protist, 2017. **168**(5): p. 495-526.
23. Riisberg, I., et al., *Seven gene phylogeny of heterokonts.* Protist, 2009. **160**(2): p. 191-204.
24. Delgehyr, N., et al., *Ependymal cell differentiation, from monociliated to multiciliated cells.* Methods Cell Biol, 2015. **127**: p. 19-35.
25. Jain, R., et al., *Temporal relationship between primary and motile ciliogenesis in airway epithelial cells.* Am J Respir Cell Mol Biol, 2010. **43**(6): p. 731-9.
26. Lechtreck, K.F., *Chlamydomonas reinhardtii as a model for flagellar assembly.* Perspectives in Phycology, 2014. **1**(1): p. 41-51.
27. Li, X., et al., *An Indexed, Mapped Mutant Library Enables Reverse Genetics Studies of Biological Processes in Chlamydomonas reinhardtii.* Plant Cell, 2016. **28**(2): p. 367-87.
28. Mittelmeier, T.M., et al., *MLT1 links cytoskeletal asymmetry to organelle placement in chlamydomonas.* Cytoskeleton (Hoboken), 2015. **72**(3): p. 113-23.
29. Holmes, J.A. and S.K. Dutcher, *Cellular asymmetry in Chlamydomonas reinhardtii.* J Cell Sci, 1989. **94 (Pt 2)**: p. 273-85.
30. Kamiya, R. and G.B. Witman, *Submicromolar levels of calcium control the balance of beating between the two flagella in demembranated models of Chlamydomonas.* J Cell Biol, 1984. **98**(1): p. 97-107.
31. Huang, B., et al., *Uniflagellar mutants of Chlamydomonas: evidence for the role of basal bodies in transmission of positional information.* Cell, 1982. **29**(3): p. 745-53.
32. Mackinder, L.C.M., et al., *A Spatial Interactome Reveals the Protein Organization of the Algal CO2-Concentrating Mechanism.* Cell, 2017. **171**(1): p. 133-147 e14.
33. Wang, Y., D.J. Stessman, and M.H. Spalding, *The CO2 concentrating mechanism and photosynthetic carbon assimilation in limiting CO2 : how Chlamydomonas works against the gradient.* Plant J, 2015. **82**(3): p. 429-48.
34. Emmer, B.T., et al., *Identification of a palmitoyl acyltransferase required for protein sorting to the flagellar membrane.* J Cell Sci, 2009. **122**(Pt 6): p. 867-74.
35. Godsel, L.M. and D.M. Engman, *Flagellar protein localization mediated by a calcium-myristoyl/palmitoyl switch mechanism.* EMBO J, 1999. **18**(8): p. 2057-65.
36. Emmer, B.T., D. Maric, and D.M. Engman, *Molecular mechanisms of protein and lipid targeting to ciliary membranes.* J Cell Sci, 2010. **123**(Pt 4): p. 529-36.
37. Mitra, M., et al., *Identification of a new chloroplast carbonic anhydrase in Chlamydomonas reinhardtii.* Plant Physiol, 2004. **135**(1): p. 173-82.

38. Heimann K, B.J., Timmermann S, Melkonian M, *The flagellar developmental cycle in algae: two types of flagellar development in uniflagellated algae.* Protoplasma, (1989 a) . . **153:**: p. 14–23.
39. Taillon, B.E., et al., *Mutational analysis of centrin: an EF-hand protein associated with three distinct contractile fibers in the basal body apparatus of Chlamydomonas.* J Cell Biol, 1992. **119**(6): p. 1613-24.
40. Piasecki, B.P. and C.D. Silflow, *The UNI1 and UNI2 genes function in the transition of triplet to doublet microtubules between the centriole and cilium in Chlamydomonas.* Mol Biol Cell, 2009. **20**(1): p. 368-78.
41. Supuran, C.T., *Carbonic anhydrases: novel therapeutic applications for inhibitors and activators.* Nat Rev Drug Discov, 2008. **7**(2): p. 168-81.
42. Kerry S. Smith, C.J., Thomas S. Whittam, James G. Ferry, *Carbonic anhydrase is an ancient enzyme widespread in prokaryotes*

Proceedings of the National Academy of Sciences, Dec 1999. **96** ((26)): p. 15184-15189.

43. Sly, W.S. and P.Y. Hu, *Human carbonic anhydrases and carbonic anhydrase deficiencies.* Annu Rev Biochem, 1995. **64**: p. 375-401.
44. Bennett, R.R. and R. Golestanian, *A steering mechanism for phototaxis in Chlamydomonas.* J R Soc Interface, 2015. **12**(104): p. 20141164.
45. Rasala, B.A., et al., *Expanding the spectral palette of fluorescent proteins for the green microalga Chlamydomonas reinhardtii.* Plant J, 2013. **74**(4): p. 545-56.
46. Gorman, D.S. and R.P. Levine, *Cytochrome f and plastocyanin: their sequence in the photosynthetic electron transport chain of Chlamydomonas reinhardi.* Proc Natl Acad Sci U S A, 1965. **54**(6): p. 1665-9.